

Article

Enhanced Properties of Micro Arc Oxidation Coating with Cu Addition on TC4 Alloy in Marine Environment

Wei Gao ¹, Jiangnan Liu ¹, Jingpeng Wei ¹, Yuhong Yao ¹, Xiqun Ma ² and Wei Yang ^{1,*}

¹ School of Materials Science and Chemical Engineering, Xi'an Technological University, Xi'an 710032, China; gaowei@xatu.edu.cn (W.G.); liujiangnan@xpu.edu.cn (J.L.); jolynn_xu@163.com (J.W.); yaoyuhong@xatu.edu.cn (Y.Y.)

² Shaanxi Key Laboratory of Biomedical Metal Materials, Northwest Institute for Nonferrous Metal Research, Xi'an 710016, China; maxiqun23@126.com

* Correspondence: yangwei_smx@163.com; Tel.: +86-029-8617-3324; Fax: +86-029-8617-3324

Abstract: By contrast with the traditional method of adding hard particles into micro arc oxidation (MAO) coating to improve its wear performance, this study introduced copper into the MAO coating on TC4 alloy by adding copper pyrophosphate to enhance the wear property in a marine environment and the antibacterial property. The results demonstrated that the MAO coating with copper pyrophosphate addition showed a porous structure, and Cu was mainly concentrated around micropores. CuO and Cu₂O were formed in this MAO coating. This MAO coating with Cu had a high bonding strength to the substrate. Although the hardness of the coating with Cu had been reduced, it could reduce the friction coefficient and enhance the wear property in simulated seawater due to the lubrication of Cu. Furthermore, this MAO coating with Cu addition had obvious antibacterial and bactericidal effects due to the antibacterial effect of Cu.

Keywords: TC4; micro arc oxidation; coating; microstructure; properties



Citation: Gao, W.; Liu, J.; Wei, J.; Yao, Y.; Ma, X.; Yang, W. Enhanced Properties of Micro Arc Oxidation Coating with Cu Addition on TC4 Alloy in Marine Environment. *Coatings* **2021**, *11*, 1168. <https://doi.org/10.3390/coatings11101168>

Academic Editor: Waseem Haider

Received: 25 August 2021

Accepted: 23 September 2021

Published: 27 September 2021

Publisher's Note: MDPI stays neutral with regard to jurisdictional claims in published maps and institutional affiliations.



Copyright: © 2021 by the authors. Licensee MDPI, Basel, Switzerland. This article is an open access article distributed under the terms and conditions of the Creative Commons Attribution (CC BY) license (<https://creativecommons.org/licenses/by/4.0/>).

1. Introduction

TC4 titanium alloy has been used in many fields due to its excellent comprehensive properties [1–4]. However, TC4 alloy has poor anti-wear property and low hardness. Some components made of TC4 alloys, such as turbine and turbofan engine blades and impellers, are limited in service life and reliability under severe wear conditions [5–8]. A large number of studies have shown that micro arc oxidation (MAO), as a common surface modification technology, can improve the anti-wear property and service life of TC4 parts [9–16]. Nonetheless, as the MAO-coated titanium components work in the seawater, they were subjected to erosion due to the porous structure of the coating surface [17]. Some hard granules such as Si₃N₄ [18], ZrO₂ [19], AlN [20], or Al₂O₃ [21] are added to reduce the friction coefficient and improve wear performance of the MAO coatings. However, adding microparticles to the basic electrolyte during the MAO process can cause solution instability. The effects of adding K₂ZrF₆ or K₂TiF₆ additives on the microstructure and properties of MAO coatings on titanium substrates were studied [22], and it was found that the MAO coating with K₂ZrF₆ addition exhibits a good anti-wear property and the best corrosion resistance. However, in the marine environment, titanium components not only need to withstand corrosion and wear, but also need to have an antibacterial property. At present, it is difficult for the prepared MAO coatings on titanium alloys to meet the collaborative improvement of protection and antifouling performance. Copper and its oxides have lubrication and excellent antibacterial properties, adding copper into MAO coatings may improve their protection and antifouling properties. Yao et al reported that the MAO coating obtained with Cu nanoparticles in the electrolyte exhibited excellent antibacterial activities [23]. Furthermore, the preparation and formation mechanism of the MAO coatings with Na₂CuY addition on TC4 alloys has been studied [24].

In our previous research, we have revealed the effect of copper pyrophosphate concentration on friction performance of MAO coating of TC4 alloy, and found that the designed coatings have excellent anti-wear property in simulated seawater. In the MAO coating with increasing copper pyrophosphate concentration in particular, the fluctuation of friction coefficient and wear scar width all decrease [25]. Therefore, in this paper, based on the above research results, the concentration of copper pyrophosphate was further increased (10 g/L), and compared with the TC4 substrate and the MAO coating without Cu, the microstructure, adhesion, mechanical property, wear resistance in the simulated seawater and antibacterial property of the MAO coating with Cu doping were systematically studied.

2. Experiment

TC4 titanium alloys (Baoji Titanium Industry Company, Baoji, China) circular specimens ($\Phi 30$ mm \times 5 mm) were used as the substrate material in this work. The compositions of this alloy were Al (5.5~6.8 wt%), V (3.5~4.5 wt%), Fe (≤ 0.30 wt%), C (≤ 0.10 wt%), N (≤ 0.05 wt%), H (≤ 0.015 wt%), O (≤ 0.20 wt%). All substrates were polished with 400#~1500# abrasive papers and then ultrasonically washed with ethanol, and finally dried in a cool air stream. Na_2SiO_3 (20 g/L), Na_2WO_4 (3 g/L), KF (4 g/L) and KOH (3 g/L) (Tianjin kemio chemical reagent Co., Ltd, Tianjin, China) was the base electrolyte with the pH value of 10. Copper pyrophosphate ($\text{Cu}_2\text{P}_2\text{O}_7$, 10 g/L) (Tianjin kemio chemical reagent Co., Ltd, Tianjin, China) with potassium sodium tartrate ($\text{NaKC}_4\text{H}_4\text{O}_6$, 15 g/L) (Tianjin kemio chemical reagent Co., Ltd., Tianjin, China) was added into the base solution. The TC4 sample was the anode, the stainless steel barrel was the cathode, and the distance between the anode and cathode was 15 cm. The MAO experiment was conducted at a constant voltage of 450 V, frequency 800 HZ, and a duty cycle of 6% for 15 min. The electrolyte temperature was maintained at 35 °C.

The surface morphologies of MAO coatings and TC4 alloy were observed by SEM + EDS (FE-SEM, S-4800, Hitachi, Japan), and the binding bond energy of the elements in MAO coating with Cu addition was tested by XPS (Axis Ultra DLD, Tsushima, Japan). Image Pro Plus software (Media Cybernetics Co., Ltd., Rockville, MD, USA) can divide different graphics into regions, and then measure the parameters, area, average radius, perimeter, optical density and other information of each region, then the average pore diameter, average pore area and porosity of MAO coatings can be calculated. The bonding strength between MAO coatings and the underlying substrate was performed by a scratch tester (WS-2005, Zhongke Kaihua Co., Ltd., Lanzhou, China). The scratch length was 5 mm, the loading rate was 60 N/min and the test load range was 0–100 N. The hardness of the coatings was obtained by using a micro-Vickers sclerometer. For each sample, more than five effective indentations were carried out. The wear test of the coatings was carried out by the ball-disk wear tester (HT-1000, Lanzhou Zhongke Kaihua, Co., Ltd., Lanzhou, China) under the simulated seawater condition. The GCr15 steel ball with 6 mm in diameter was in the form of a pair of grinding balls (wear resistance test). The load and speed were 200 g and 224 r/min, respectively. The friction radius and wear time were 5 mm and 30 min, respectively. The antibacterial property of the micro arc oxidation coating was evaluated by observing the bactericidal effect on *Staphylococcus aureus*. Firstly, the washed bacterial solution was moved into the 12 orifice plate of 1500 μm by a pipette gun. Then it was put into a constant temperature shaking table for culture at 37 °C for 3 days. In order to ensure the uniform distribution of bacteria on the MAO coating, the rotating speed of the shaking table was set to 160 rpm. After the culture, the optical density (OD) was measured by microplate reader (Multiskan MK3, Thermo Fisher, Waltham, MA, USA).

3. Results and Discussion

Figure 1 shows surface morphologies of TC4 and the MAO coatings prepared in various solutions. As shown in Figure 1a, the surface of TC4 without MAO coating is smooth and flat. It mainly contains Ti, Al and V elements, and each element is evenly distributed. As shown in Figure 1b, the MAO coating without Cu has many crater-shaped

discharge channels, showing some volcanic bulges. The roughness of this coating is $1.95 \mu\text{m}$. The average aperture and area is 0.66 and $0.76 \mu\text{m}^2$, respectively. This coating is mainly composed of Ti, Si and O elements, and Ti comes from the TC4 substrate, O and Si from the electrolyte. Solute ions are strongly involved in the formation of MAO coating, which is consistent with the literature [26]. It can be obtained by Image Pro Plus software that the average aperture and area of MAO coating with Cu is $0.91 \mu\text{m}$ and $1.08 \mu\text{m}^2$, respectively, and the roughness of this film is $2.19 \mu\text{m}$, shown in Figure 1c. The higher surface roughness may be related to the more intense micro arc discharge process caused by the addition of copper pyrophosphate. The EDS results of the coating are shown in Figure 1d. It is found that Cu element is concentrated around the pore. Wang et al. obtained similar research results [27]. It is known that the growth of MAO coating is a cyclic process of breakdown and condensation [28–30]. Due to a low melting point of Cu, it is preferentially attached to the coating by the strong discharge. As a result, the enrichment of copper in turn led to poor insulation in this region and preferential breakdown discharge.

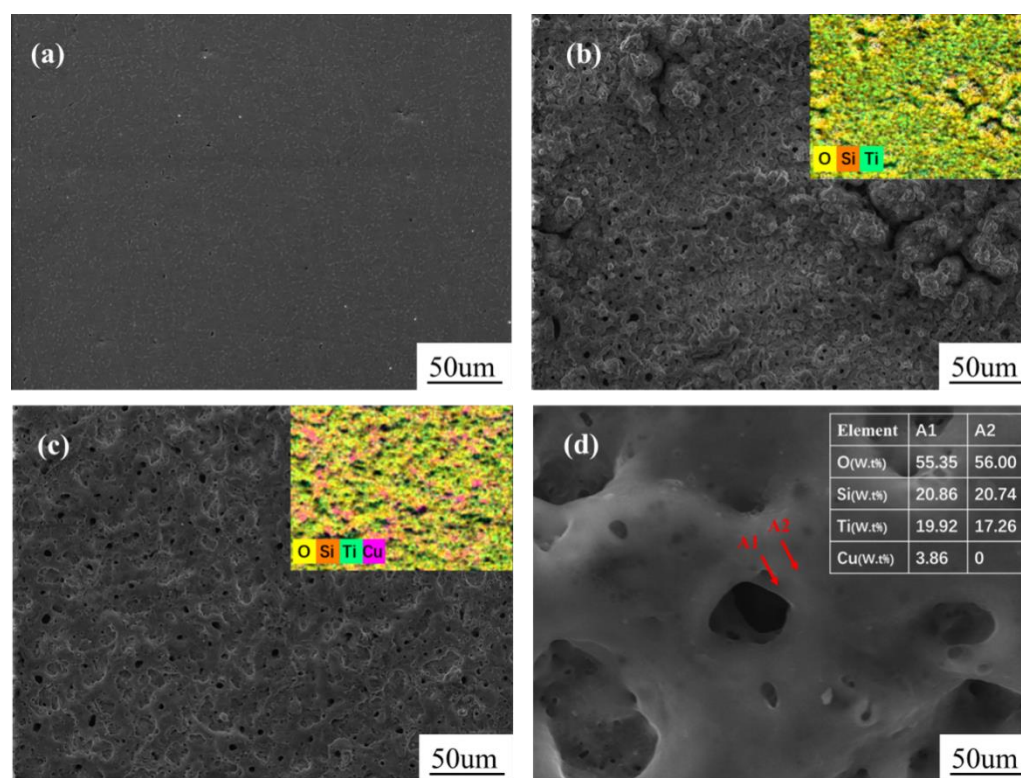


Figure 1. Scanning electron microscopy (SEM) images and energy-dispersive X-ray spectroscopy (EDS) of TC4 $\times 1000$ (a), micro arc oxidation (MAO) coatings without Cu $\times 1000$ (b); MAO coatings with copper pyrophosphate (c) and (d) $\times 10,000$.

XPS spectra and high-resolution XPS spectra of MAO-with Cu coating show mainly O, Si, Ti, and Cu elements, Figure 2a. The binding energy of Si2p peak at 102.70 eV indicates the existence of SiO_2 . High-resolution XPS spectra for Cu 2p of ceramic oxide coating consist of four characteristic peaks, indicating that both Cu_2O and CuO are present to ceramic oxide coating. However, Li et al report that Cu in MAO coatings exists mainly in the form of Cu_2O [24]. This is related to the different ways of introducing Cu into MAO coatings and the different electrical parameters during the MAO process. The Ti 2p spectrum (Figure 2b) includes peaks at 458.3 eV and 464.0 eV , which are attributed to typical binding energies of TiO_2 . Obviously, as copper pyrophosphate was added to MAO base solution, the microhardness of the oxide film was reduced due to the formation of copper oxide.

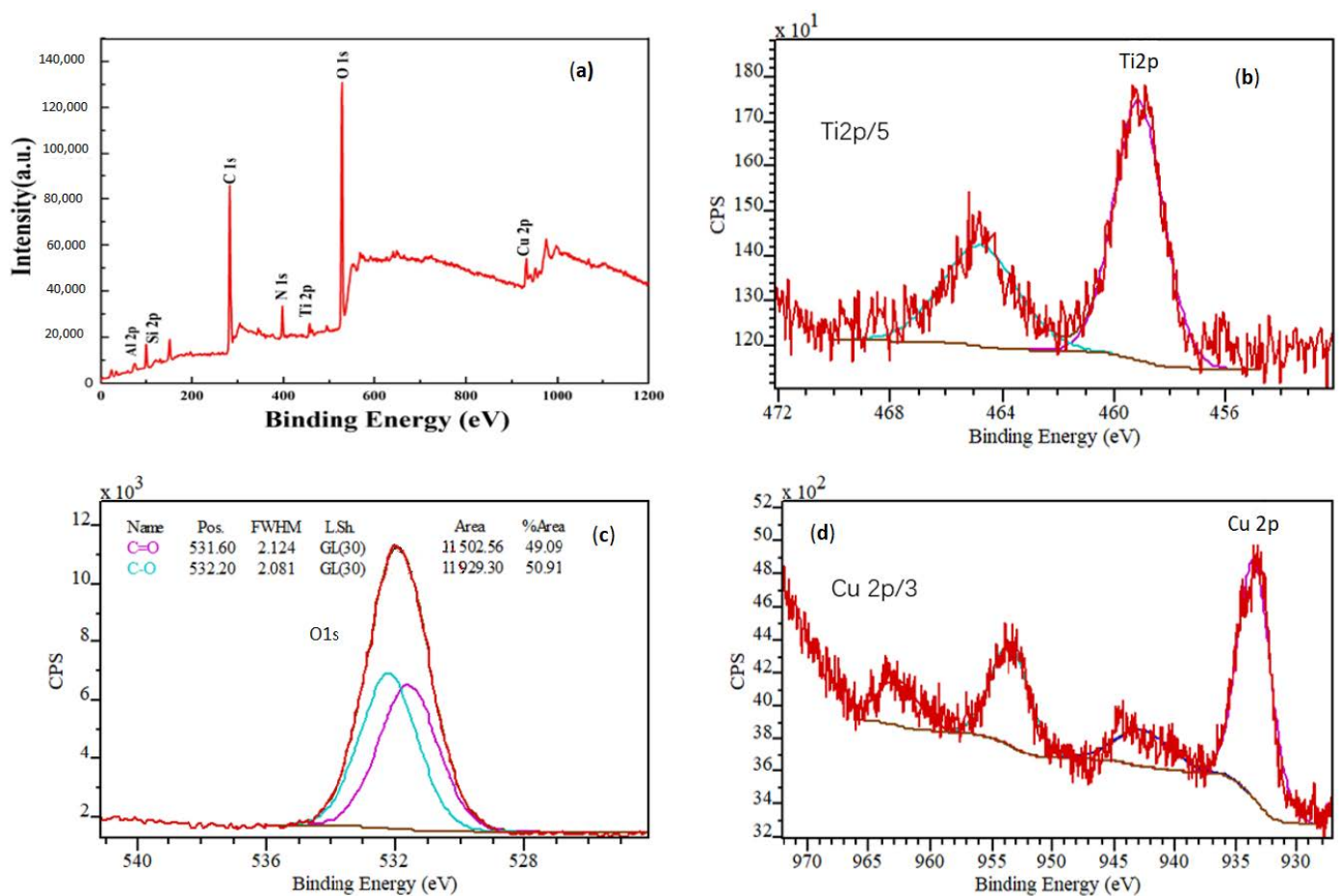


Figure 2. X-ray photoelectron spectroscopy (XPS) spectra and high-resolution XPS spectra of MAO coating with Cu: (a) survey; (b) Ti 2p; (c) O 1s; (d) Cu 2p.

The bonding strength between the MAO coating and substrate affects its performance to a great extent, and obtaining high hardness is an effective way to improve the wear resistance of the coating. The bonding force and hardness values of TC4, MAO without Cu, and MAO coating with Cu are shown in Figure 3. The bonding force of MAO coating without Cu and MAO coating with Cu was 84.58 and 84.65 N, respectively. This high bonding strength of the high coating substrate has exceeded the bonding strength of the hard film on tool, which is due to the metallurgical bonding between coating and substrate [31]. The microhardness values of TC4, MAO coating without Cu, and MAO coating with Cu were separately 363 HV, 558 HV and 384 HV, respectively. Obviously, the microhardness of the coating decreased after the addition of copper pyrophosphate due to a low hardness value of copper oxide.

The friction curves of TC4 and two MAO coatings is shown in Figure 4a. The friction coefficient of the TC4 substrate was high and fluctuated greatly. Compared with the substrate, the friction coefficient of the MAO coating without Cu changed low, but its fluctuations are still evident. The friction coefficient of the MAO coating with Cu was smooth and the fluctuation is very small in the simulated seawater, showing excellent tribological behavior, which was due to the self-lubrication of Cu in the MAO coating. Figure 4b illustrates the wear track (about 561 μm) of the TC4 alloy, showing furrow wear property. Fe element from the grinding ball appeared in the wear track, and the distribution of O at the wear track was obvious, indicating the oxidation phenomenon occurred during the wear process in the simulated seawater. As shown in Figure 4c,d, the wear tracks of the two MAO coatings were 474 μm and 373 μm , respectively. It could be found that smooth and continuous oxide glaze layers were formed, which is characteristic of adhesive wear.

For the MAO coating with Cu in particular, the existence of Cu had a self-lubricating effect and improved the tribological property in simulated seawater.

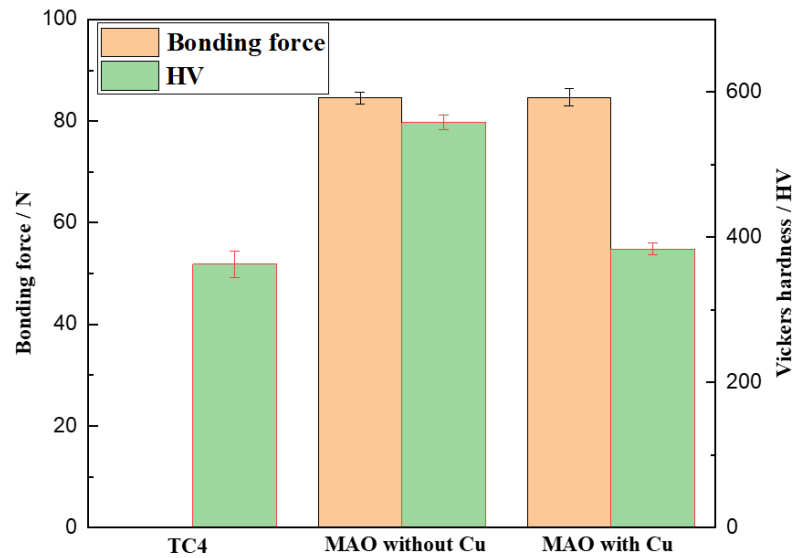


Figure 3. Hardness and bonding force of TC4, MAO coating with Cu, and MAO coating without Cu.

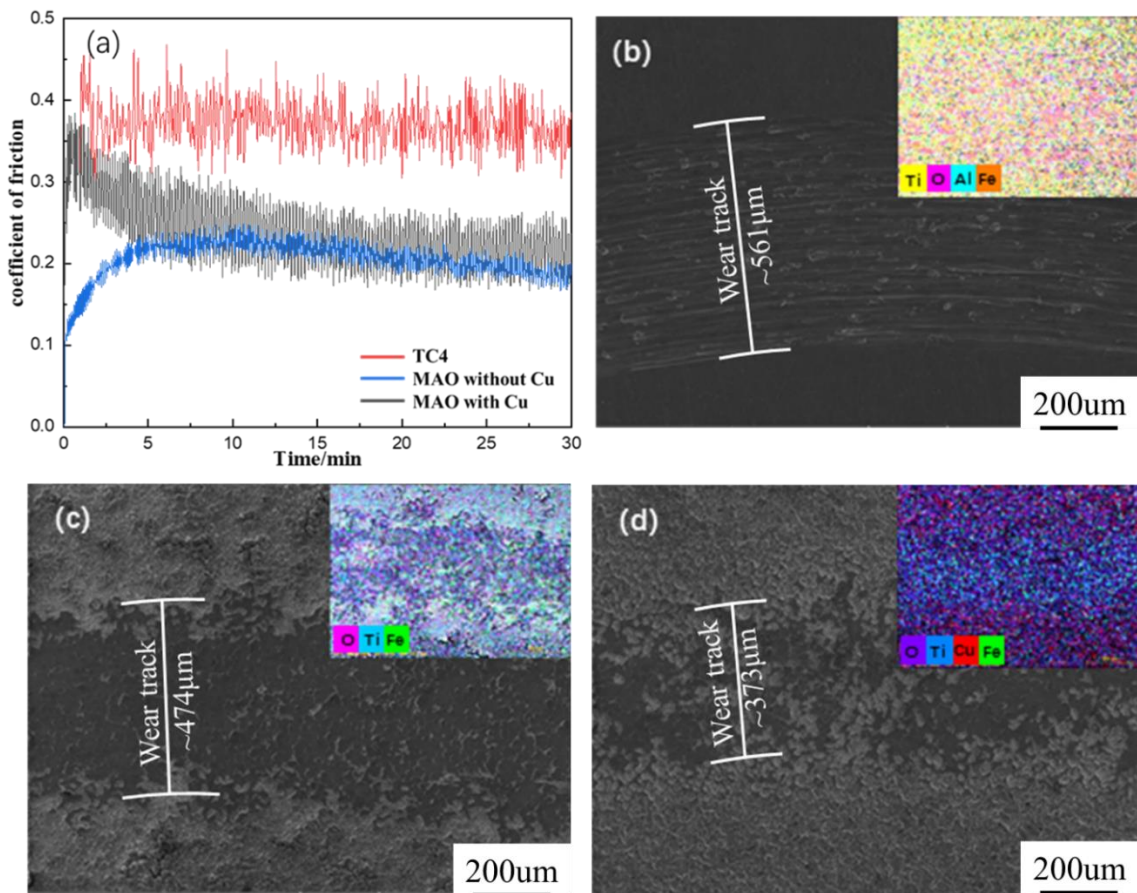


Figure 4. Friction coefficient curves and wear morphologies of Ti substrate and coated samples, (a) friction coefficient (b) TC4, (c) MAO coating without Cu, and (d) MAO coating with Cu.

Figure 5 shows SEM morphologies of *Staphylococcus aureus* cultured for 3 days on TC4 substrate and MAO-coated samples. The number of *Staphylococcus aureus* on the

MAO-coated sample increased significantly compared with the substrate, which was due to its porous microstructure and it being more conducive to the adhesion and increment of bacteria. Only a small amount of *Staphylococcus aureus* adhered on the MAO coating with Cu, and the bacterial aggregation significantly decreased. Yao et al. have found that both direct contact killing and an ion release antibacterial mechanism play a major role in the antibacterial activities of Cu [23]. Furthermore, the OD value of *Staphylococcus aureus* cultured in MAO coating with Cu for 3 days was 0.410, which was lower than the TC4 substrate (1.084) and the MAO coating without Cu (1.180), showing that this oxide coating with Cu had an obvious antibacterial and bactericidal effect. So, the authors believed that the porous surface of the MAO coatings made it easy for the bacteria to adhere and the antibacterial property became bad, but copper in the MAO coating could effectively improve the antibacterial property.

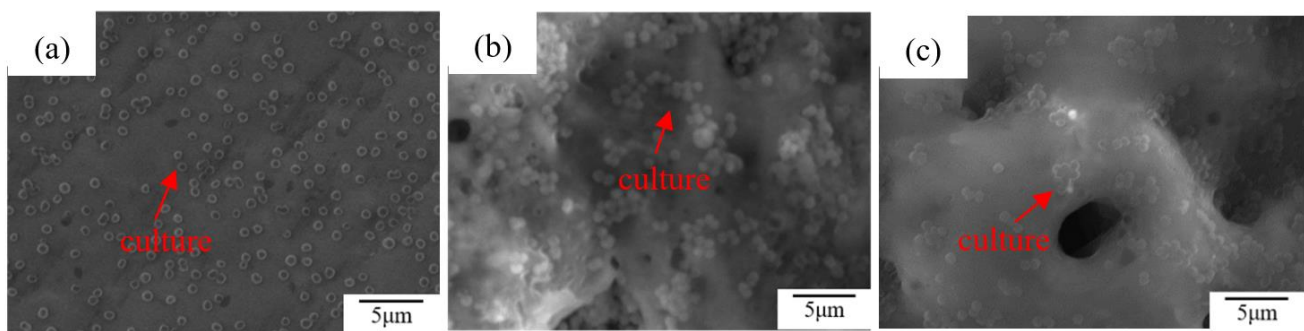


Figure 5. SEM morphologies of *Staphylococcus aureus* cultured for 3 days on TC4 substrate and MAO-coated samples, (a) TC4, (b) MAO coating without Cu, and (c) MAO coating with Cu.

4. Conclusions

1. The MAO coating with Cu on TC4 alloy was prepared in the base electrolyte with copper pyrophosphate addition, in the form of Cu_2O and CuO . This coating still showed a porous structure, and Cu was mainly concentrated around micropores.
2. The addition of Cu increases the porosity in the MAO coating, having a high bonding strength with the substrate. Although the addition of Cu reduces the hardness of the MAO coating, its friction coefficient was stable and low, and the wear track width was the smallest, which was due to the lubrication of Cu.
3. Although the porous characteristics of the MAO coating make it easy for bacteria to attach, this MAO coating with Cu demonstrated excellent antibacterial property due to the antibacterial activities of Cu.

Author Contributions: Conceptualization, W.G. and J.L.; methodology, J.W.; software, Y.Y.; validation, X.M.; formal analysis, W.Y.; investigation, W.Y.; resources, W.G. and J.L.; data curation, W.G. and J.L.; writing—original draft preparation, W.G. and J.L.; writing—review and editing, Y.Y.; visualization, X.M.; supervision X.M.; project administration, W.Y.; funding acquisition, W.Y. All authors have read and agreed to the published version of the manuscript.

Funding: This work was financially supported by the Natural Science Foundation of China (Grant No. 52071252), Key Research and Development Plan of Shaanxi Province-industrial Project (Grant No. 2021GY-208 and 2021ZDLSF03-11).

Institutional Review Board Statement: Not applicable.

Informed Consent Statement: Not applicable.

Data Availability Statement: Data is contained within the article.

Conflicts of Interest: The authors declare no conflict of interest.

References

1. Yan, S.K.; Song, G.L.; Li, Z.X.; Wang, H.N.; Zheng, D.J. A state-of-the-art review on passivation and biofouling of Ti and its alloys in marine environments. *Mater. Sci. Technol.* **2018**, *34*, 421–435. [[CrossRef](#)]
2. Yang, W.; Gao, Y.; Guo, P.; Xu, D.P.; Hu, L.; Wang, A.Y. Adhesion, biological corrosion resistance and biotribological properties of carbon films deposited on MAO coated Ti substrates. *J. Mech. Behav. Biomed* **2020**, *101*, 103448. [[CrossRef](#)] [[PubMed](#)]
3. Wake, H.; Takimoto, T.; Takayanagi, H.; Ozawa, K.; Kadoi, H.; Okochi, M.; Matsunaga, T. Development of an Electrochemical Antifouling System for Seawater Cooling Pipelines of Power Plants Using Titanium. *Biotechnol. Bioeng.* **2010**, *95*, 468–473. [[CrossRef](#)] [[PubMed](#)]
4. Jing, R.; Liang, S.X.; Liu, C.Y.; Ma, M.Z.; Zhang, X.Y.; Liu, R.P. Structure and mechanical properties of Ti–6Al–4V alloy after zirconium addition. *Mater. Sci. Eng. A* **2012**, *552*, 295–300. [[CrossRef](#)]
5. Zhang, T.G.; Zhuang, H.F.; Zhang, Q.; Yao, B.; Yang, F. Influence of Y₂O₃ on the microstructure and tribological properties of Ti-based wear-resistant laser-clad layers on TC4 alloy. *Ceram. Int.* **2020**, *46*, 13711–13723. [[CrossRef](#)]
6. Shokouhfar, M.; Allahkaram, S.R. Effect of incorporation of nanoparticles with different composition on wear and corrosion behavior of ceramic coatings developed on pure titanium by micro arc oxidation. *Surf. Coat. Technol.* **2017**, *309*, 767–778. [[CrossRef](#)]
7. Ao, N.; Liu, D.X.; Wang, S.X.; Zhao, Q.; Zhang, X.H. Microstructure and Tribological Behavior of a TiO₂/hBN Composite Ceramic Coating Formed via Microarc Oxidation of Ti–6Al–4V Alloy. *J. Mater. Sci. Technol.* **2016**, *32*, 1071–1076. [[CrossRef](#)]
8. Zhou, H.Y.; Shi, X.L.; Lua, G.C.; Chen, Y.; Yang, Z.Y.; Wu, C.H.; Xue, Y.E. Friction and wear behaviors of TC4 alloy with surface microporous channels filled by Sn–Ag–Cu and Al₂O₃ nanoparticles. *Surf. Coat. Technol.* **2020**, *384*, 125552. [[CrossRef](#)]
9. Yang, W.; Gao, Y.; Xu, D.P.; Zhao, J.; Ke, P.L.; Wang, A.Y. Bactericidal abilities and in vitro properties of diamond-like carbon films deposited onto MAO-treated titanium. *Mater. Lett.* **2019**, *244*, 155–158. [[CrossRef](#)]
10. Fang, Y.J.; Jiang, X.S.; Song, T.F.; Mo, D.F.; Luo, Z.P. Pulsed laser welding of Ti–6Al–4V titanium alloy to AISI316L stainless steel using Cu/Nb bilayer. *Mater. Lett.* **2019**, *244*, 163–166. [[CrossRef](#)]
11. Fazel, M.; Salimijazi, H.R.; Golozar, M.A.; Garsivazjazi, M.R. A comparison of corrosion, tribocorrosion and electrochemical impedance properties of pure Ti and Ti6Al4V alloy treated by micro-arc oxidation process. *Appl. Surf. Sci.* **2015**, *324*, 751–756. [[CrossRef](#)]
12. Vangolu, Y.; Arslan, E.; Totik, Y.; Demirci, E.; Alsarar, A. Optimization of the coating parameters for micro-arc oxidation of Cp-Ti. *Surf. Coat. Technol.* **2010**, *205*, 1764–1773. [[CrossRef](#)]
13. Zhou, G.H.; Ding, H.Y.; Zhang, Y.; Liu, A.H.; Lin, Y.B.; Zhu, Y.F. Fretting Wear Study on Micro-Arc Oxidation TiO₂ Coating on TC4 Titanium Alloys in Simulated Body Fluid. *Tribol. Lett.* **2010**, *40*, 319–326. [[CrossRef](#)]
14. Cheng, Z.H.; Yang, W.; Xu, D.P.; Wu, S.K.; Yao, X.F.; Lv, Y.K.; Chen, J. Improvement of high temperature oxidation resistance of micro arc oxidation coated AlTiNbMo_{0.5}Ta_{0.5}Zr high entropy alloy. *Mater. Lett.* **2019**, *262*, 127192. [[CrossRef](#)]
15. Lin, R.Z.X.M.; Zhou, P.; Zou, J.J.; Han, P.J.; Wang, Z.H.; Tang, B. Surface damage mitigation of TC4 alloy via micro arc oxidation for oil and gas exploitation application: Characterizations of microstructure and evaluations on surface performance. *Appl. Surf. Sci.* **2018**, *436*, 467–476.
16. Narayanan, T.S.N.S.; Park, I.S.; Lee, M.H. Strategies to improve the corrosion resistance of microarc oxidation (MAO) coated magnesium alloys for degradable implants: Prospects and challenges. *Prog. Mater. Sci.* **2014**, *60*, 1–71. [[CrossRef](#)]
17. Wang, S.; Xie, F.; Wu, X.; Chen, L. CeO₂ doped Al₂O₃ composite ceramic coatings fabricated on γ-TiAl alloys via cathodic plasma electrolytic deposition. *J. Alloys Compd.* **2019**, *788*, 632–638. [[CrossRef](#)]
18. Aliofkhaezai, M.; Rouhaghdam, A.S.; Shahrahi, T. Abrasive wear behaviour of Si₃N₄/TiO₂ nanocomposite coatings fabricated by plasma electrolytic oxidation. *Surf. Coat. Technol.* **2010**, *205*, S41–S46. [[CrossRef](#)]
19. Wang, S.Q.; Xie, F.Q.; Wu, X.Q.; Ma, Y.; Du, H.X.; Wu, G. Cathodic plasma electrolytic deposition of ZrO₂/YSZ doped Al₂O₃ ceramic coating on TiAl alloy. *Ceram. Int.* **2019**, *45*, 18899–18907. [[CrossRef](#)]
20. Yang, W.; Wu, S.K.; Xu, D.P.; Gao, W.; Yao, Y.H.; Guo, Q.Q.; Chen, J. Preparation and performance of alumina ceramic coating doped with aluminum nitride by micro arc oxidation. *Ceram. Int.* **2020**, *46*, 17112–17116. [[CrossRef](#)]
21. Wang, S.Q.; Xie, F.Q.; Wu, X.Q.; Lv, T.; Ma, Y. Microstructure and high temperature oxidation behavior of the Al₂O₃ CPED coating on TiAl alloy. *J. Alloys Compd.* **2020**, *828*, 154271. [[CrossRef](#)]
22. Yang, W.; Xu, D.; Guo, Q.; Chen, T.; Chen, J. Influence of electrolyte composition on microstructure and properties of coatings formed on pure Ti substrate by micro arc oxidation. *Surf. Coat. Technol.* **2018**, *349*, 522–528. [[CrossRef](#)]
23. Yao, X.H.; Zhang, X.Y.; Wu, H.B.; Tian, L.H.; Ma, Y.; Tang, B. Microstructure and antibacterial properties of Cu-doped TiO₂ coating on titanium by micro-arc oxidation. *Appl. Surf. Sci.* **2014**, *292*, 944–947. [[CrossRef](#)]
24. Li, G.Q.; Wang, Y.P.; Qiao, L.P.; Zhao, R.F.; Zhang, S.F.; Zhang, R.F.; Chen, C.M.; Li, X.Y.; Zhao, Y. Preparation and formation mechanism of copper incorporated micro-arc oxidation coatings developed on Ti–6Al–4V alloys. *Surf. Coat. Technol.* **2019**, *375*, 74–85. [[CrossRef](#)]
25. Wei, J.P.; Gao, W.; Cheng, Z.H.; Yao, Y.H.; Jin, Y.H.; Chen, J.; Yang, W. Effect of copper pyrophosphate concentration on friction performance of micro arc oxidation layer of TC4 alloy. *Trans. Mater. Heat Treat.* **2021**, *42*, 162–167. (In Chinese) [[CrossRef](#)]
26. Yang, W.; Xu, D.P.; Yao, X.F.; Wang, J.L.; Chen, J. Stable preparation and characterization of yellow micro arc oxidation coating on magnesium alloy. *J. Alloys Compd.* **2018**, *745*, 609–616. [[CrossRef](#)]

27. Wang, J.L.; Yang, W.; Xu, D.P.; Yao, X.F. The effects of $K_2TiO(C_2O_4)_2$ addition in electrolyte on the microstructure and tribological behavior of micro-arc oxidation coatings on aluminium alloy. *Acta Metall. Sin. (Engl. Lett.)* **2017**, *30*, 1109–1118. [[CrossRef](#)]
28. Wang, W.Q.; Zheng, X.C.; Yu, F.Y.; Li, Y.D.; Xue, X.D.; Qi, M.; Li, Y. Formation and cytocompatibility of a hierarchical porous coating on Ti-20Zr-10Nb-4Ta alloy by micro-arc oxidation. *Surf. Coat. Technol.* **2020**, *404*, 126471. [[CrossRef](#)]
29. Liu, S.M.; Li, B.E.; Liang, C.Y.; Wang, H.S.; Qiao, Z.X. Formation mechanism and adhesive strength of a hydroxyapatite/TiO₂ composite coating on a titanium surface prepared by micro-arc oxidation. *Appl. Surf. Sci.* **2016**, *362*, 109–114. [[CrossRef](#)]
30. Shokouhfar, M.; Allahkaram, S.R. Formation mechanism and surface characterization of ceramic composite coatings on pure titanium prepared by micro-arc oxidation in electrolytes containing nanoparticles. *Surf. Coat. Technol.* **2016**, *291*, 396–405. [[CrossRef](#)]
31. Hong, M.H.; Lee, D.H.; Kim, K.M.; Lee, Y.K. Study on bioactivity and bonding strength between Ti alloy substrate and TiO₂ film by micro-arc oxidation. *Thin Solid Films* **2011**, *519*, 7065–7070. [[CrossRef](#)]